

Dynamically enhanced $B \rightarrow K^*\pi$ decays in perturbative QCD

Yong-Yeon Keum

EKEN Lab. Department of Physics

Nagoya University, Nagoya 464-8602 Japan

Email: yykeum@eken.phys.nagoya-u.ac.jp

(Dated: November 6, 2018)

We investigate the $B \rightarrow K^*\pi$ decays, one of hardly understandable processes among charmless B-meson decays, within the perturbative QCD method. Owing to the dynamically enhanced mechanism in PQCD, we obtain large branching ratios and large direct CP asymmetries: $Br(B^0 \rightarrow K^{*\pm}\pi^\mp) = (9.1^{+4.9+0.3}_{-3.9-0.2}) \times 10^{-6}$, $Br(B^\pm \rightarrow K^{*0}\pi^\pm) = (10.0^{+5.3}_{-3.5} \pm 0.0) \times 10^{-6}$; $A_{cp}(B^0 \rightarrow K^{*\pm}\pi^\mp) = (-19.2^{+0.5}_{-1.7})\%$, and $A_{cp}(B^\pm \rightarrow K^{*0}\pi^\pm) = (-43.7^{+4.0}_{-4.2})\%$. The branching ratios are consistent with experimental data and large direct CP violation effects will be tested by near future experimental measurements in Asymmetric B-factory.

PACS numbers: 13.25.Hw, 11.30.Er, 12.38.Bx, 14.40.Nd

The predictive power of the perturbative QCD (pQCD) approach has been demonstrated successfully in exclusive 2-body B-meson decays, especially charmless B-meson processes [1, 2, 3, 4, 5, 6, 7, 8] which is based on k_T factorization theorem [9]. This is a modified version of the pQCD theory for exclusive processes[10]. The idea is to separate hard scattering kernels from a high-energy QCD process, which are calculable in a perturbative way. Nonperturbative parts are organized into universal hadron distribution amplitudes, which can be determined from experimental data. By introducing parton transverse momenta k_\perp , we can generate naturally the Sudakov suppression effect due to the resummation of large double logarithms $Exp[-\frac{\alpha_s C_F}{4\pi} \ln^2(\frac{Q^2}{k_\perp^2})]$, which suppress the long-distance contributions in the small k_\perp region and give a sizable average $\langle k_\perp^2 \rangle \sim \bar{\Lambda} M_B$. This can resolve the end point singularity problem and allow the applicability of pQCD to exclusive B-meson decays. We found that almost all of the contributions to the matrix element come from the integration region where $\alpha_s/\pi < 0.3$ and the perturbative treatment can be justified.

In the pQCD approach, we can predict the contribution of non-factorizable term and annihilation diagram on the same basis as the factorizable one. A folklore for annihilation contributions is that they are negligible compared to W-emission diagrams due to helicity suppression. However the operators $O_{5,6}$ with helicity structure $(S - P)(S + P)$ are not suppressed and give dominant imaginary values, which is the main source of strong phase in the pQCD approach.

An alternative method to exclusive B meson decays is QCD-factorization approach (QCDF)[11], which is based on collinear factorization theorem.

For some modes, such as the $B \rightarrow K\pi$ decays, the difference between the pQCD and QCDF approaches may not be significant. As explained in ref.[2], the typical hard scattering scale is about 1.5 GeV. Since the RG evolution of the Wilson coefficients $C_{4,6}(t)$ increase drastically as $t < M_B/2$, while that of $C_{1,2}(t)$ remain almost constant, we can get a large enhancement effects from

both wilson coefficients and matrix elements in pQCD.

In general the amplitude can be expressed as

$$Amp \sim [a_{1,2} \pm a_4 \pm m_0^{P,V}(\mu)a_6] \cdot \langle K\pi|O|B \rangle \quad (1)$$

with the chiral factors $m_0^P(\mu) = m_P^2/[m_1(\mu) + m_2(\mu)]$ for pseudoscalar meson and $m_0^V = m_V$ for vector meson. To accommodate the $B \rightarrow K\pi$ data in the factorization and QCD-factorization approaches, one relies on the chiral enhancement by increasing the mass m_0 to as large values about 3 GeV at $\mu = m_b$ scale. So two methods accomodate large branching ratios of $B \rightarrow K\pi$ and it is difficult for us to distinguish two different methods in $B \rightarrow PP$ decays. In addition, the direct CP asymmetries in $B \rightarrow K\pi$ decays are not large enough to distinguish the two approaches after taking into account the theoretical uncertainties.

However the difference can be detected in the direct CP asymmetry of $B^0 \rightarrow \pi^\pm\pi^\mp$ process because of the different power counting rules and the branching ratios of in $B \rightarrow PV$ modes since there is no chiral enhanced factor in LCDAs of the vector meson. Due to the different power counting rules of the QCDF and pQCD approaches, based on collinear and k_T factorizations, respectively, the vertex correction is the leading source of the strong phase in the former, and the annihilation diagram is in the latter. The strong phases derived from the above two sources are opposite in sign, and the latter has a large magnitude. This is the reason QCDF prefers a small and positive CP asymmetry $C_{\pi\pi}$ [12], while pQCD prefers a large and negative $C_{\pi\pi} \sim -30\%$ [2, 8].

We can test whether dynamical enhancement or chiral enhancement is responsible for the large $B \rightarrow K\pi$ branching ratios by measuring the $B \rightarrow \phi K^{(*)}$ modes. In these modes penguin contributions dominate, such that their branching ratios are insensitive to the variation of the unitarity angle ϕ_3 . According to recent works within QCDF[13], the branching ratio of $B \rightarrow \phi K$ is $(2 - 7) \times 10^{-6}$ including 30% annihilation contributions in real part of amplitudes within QCD-factorization approach. However pQCD predicts 10×10^{-6} [5] with mostly pure imaginary annihilation contributions. For

$B \rightarrow \phi K^*$ decays, QCDF gets about 9×10^{-6} [14], but pQCD have 15×10^{-6} [6]. Because of these relatively small branching ratios for $B \rightarrow PV$ and VV decays in QCD-factorization approach, they can not globally fit the experimental data for $B \rightarrow PP, VP$ and VV modes simultaneously with same sets of free parameters (ρ_H, ϕ_H) and (ρ_A, ϕ_A) [16]. To explain large branching ratios of $B \rightarrow VP$ modes, they have to break the universality of free parameter sets with $\rho_{H,A} \geq 1$ and finally lost the predictive power.

In this letter we investigate the more complicated $B \rightarrow K^*\pi$ processes, which contain both tree and penguin contributions, while $B \rightarrow \phi K^{(*)}$ is a pure penguin process. It is well known that it is very difficult to explain the observed $B \rightarrow K^*\pi$ branching ratios using the factorization assumption (FA) [15] and QCDF[16]: the experimental measurements are much larger than the theoretical predictions.

The reason is as follows. The measured $Br(B \rightarrow K^*\pi)$ are roughly the same as $Br(B \rightarrow K\pi) \sim 2 \times 10^{-5}$. However, the penguin operators $O_{5,6}$ contribute to the latter, but not to the former. Due to the loss of this important piece of contributions, the predicted $Br(B \rightarrow K^*\pi)$ become a quarter of the predicted $Br(B \rightarrow K\pi)$. The same difficulty has been encountered in the $B \rightarrow \rho\pi$ decays, where the vector meson is replaced by a ρ meson [4]. This controversy remains, no matter how the angle ϕ_3 is varied [17]. Hence, the $B \rightarrow K^*\pi$ decays is worth of an intensive study.

We shall evaluate the branching ratios of the following modes,

$$\begin{aligned} B^\pm &\rightarrow K^{*0}\pi^\pm, & B_d^0 &\rightarrow K^{*\pm}\pi^\mp, \\ B^\pm &\rightarrow K^{*\pm}\pi^0, & B_d^0 &\rightarrow K^{*0}\pi^0, \end{aligned} \quad (2)$$

and the CP asymmetries, for instance, $f = K^{*+}\pi^-$

$$A_{CP} = \frac{\text{Br}(\bar{B}_d^0 \rightarrow \bar{f}) - \text{Br}(B_d^0 \rightarrow f)}{\text{Br}(\bar{B}_d^0 \rightarrow \bar{f}) + \text{Br}(B_d^0 \rightarrow f)}, \quad (3)$$

as functions of the unitarity angle ϕ_3 . It will be shown that penguin and annihilation amplitudes in the $B \rightarrow K^*\pi$ decays are greatly enhanced by Wilson evolutin effects. There is also small enhancement from the K^* meson wave functions, which are more asymmetric than the kaon wave functions, and from the K^* meson decay constant f_{K^*} , which is larger than the kaon decay constant f_K . It turns out that these enhancements compensate the loss of the $O_{5,6}$ contributions, and that PQCD predictions are in agreement with the data.

The decay rates of $B \rightarrow K^*\pi$ have the expressions,

$$\Gamma = \frac{G_F^2 M_B^3}{128\pi} |\mathcal{A}|^2. \quad (4)$$

The decay amplitudes \mathcal{A} for the different modes are writ-

ten as

$$\begin{aligned} \mathcal{A}(K^{*0}\pi^+) &= f_{K^*} V_t^* F_e^{P(d)} + V_t^* \mathcal{M}_e^{P(d)} + f_B V_t^* F_a^{P(u)} \\ &\quad + V_t^* \mathcal{M}_a^{P(u)} - f_B V_u^* F_a^T - V_u^* \mathcal{M}_a^T, \end{aligned} \quad (5)$$

$$\begin{aligned} \mathcal{A}(K^{*+}\pi^-) &= f_{K^*} V_t^* F_e^{P(u)} + V_t^* \mathcal{M}_e^{P(u)} + f_B V_t^* F_a^{P(d)} \\ &\quad + V_t^* \mathcal{M}_a^{P(d)} - f_{K^*} V_u^* F_e^T - V_u^* \mathcal{M}_e^T, \end{aligned} \quad (6)$$

$$\begin{aligned} \sqrt{2}\mathcal{A}(K^{*+}\pi^0) &= f_{K^*} V_t^* F_e^{P(u)} + V_t^* \mathcal{M}_e^{P(u)} + f_B V_t^* F_a^{P(u)} \\ &\quad + V_t^* \mathcal{M}_a^{P(u)} + f_\pi V_t^* F_{eK}^P + V_t^* \mathcal{M}_{eK}^P \\ &\quad - f_{K^*} V_u^* F_e^T - V_u^* \mathcal{M}_e^T - f_B V_u^* F_a^T \\ &\quad - V_u^* \mathcal{M}_a^T - f_\pi V_u^* F_{eK}^T - V_u^* \mathcal{M}_{eK}^T, \end{aligned} \quad (7)$$

$$\begin{aligned} \sqrt{2}\mathcal{A}(K^{*0}\pi^0) &= f_{K^*} V_t^* F_e^{P(d)} + V_t^* \mathcal{M}_e^{P(d)} + f_B V_t^* F_a^{P(d)} \\ &\quad + V_t^* \mathcal{M}_a^{P(d)} + f_\pi V_t^* F_{eK}^P + V_t^* \mathcal{M}_{eK}^P \\ &\quad - f_\pi V_u^* F_{eK}^T - V_u^* \mathcal{M}_{eK}^T, \end{aligned} \quad (8)$$

to which $\mathcal{A}(K^{*0}\pi^-)$, $\mathcal{A}(K^{*-}\pi^+)$, $\sqrt{2}\mathcal{A}(K^{*-}\pi^0)$, and $\sqrt{2}\mathcal{A}(\bar{K}^{*0}\pi^0)$ are identical, respectively, but with the the product V_t^* (V_u^*) of the CKM matrix elements replaced by V_t (V_u).

The detail expression of analytic formulas for all amplitudes ($F_i^{T,P}$ and $M_i^{T,P}$) will be presented elsewhere[19]. In the above expressions f_B is the B meson decay constant. The notations F represent factorizable contributions (form factors), and \mathcal{M} represent nonfactorizable (color-suppressed) contributions. The subscripts a and e denote the annihilation and W-emission topology, respectively. The superscript $P(T)$ denotes contributions from the penguin (Tree) operators. $F_{a(e)}^T$, associated with the time-like $K^*-\pi$ form factor ($B \rightarrow \pi$ form factor), and $\mathcal{M}_{a(e)}^T$ are from the operators $O_{1,2}^{(u)}$. The factorizable contribution F_{eK}^P (F_{eK}^T) is associated with the $B \rightarrow K^*$ form factor from the penguin (tree) operators, and \mathcal{M}_{eK}^P (\mathcal{M}_{eK}^T) is the corresponding nonfactorizable contribution.

In our numerical analysis, we use $G_F = 1.16639 \times 10^{-5}$ GeV⁻², the Wolfenstein parameters $\lambda = 0.2196$, $A = 0.819$, and $R_b = 0.38_{-0.06}^{+0.10}$ for the CKM matrix elements, the masses $M_B = 5.28$ GeV and $M_{K^*} = 0.892$ GeV, and

TABLE I: Contribution to the $B_u^+ \rightarrow K^{*+}\pi^0$ decay from each form factor and nonfactorizable amplitude.

$f_{K^*} F_e^T$	-1.202×10^{-1}
$f_{K^*} F_e^P$	4.424×10^{-3}
$f_B F_a^T$	$-3.521 \times 10^{-2} + i 4.422 \times 10^{-3}$
$f_B F_a^P$	$2.002 \times 10^{-3} - i 2.076 \times 10^{-3}$
M_e^T	$-4.369 \times 10^{-3} + i 5.317 \times 10^{-3}$
M_e^P	$1.733 \times 10^{-4} - i 2.612 \times 10^{-4}$
M_a^T	$-4.413 \times 10^{-4} + i 1.297 \times 10^{-3}$
M_a^P	$-3.355 \times 10^{-5} - i 4.591 \times 10^{-6}$
$f_\pi F_{eK}^T$	-1.089×10^{-2}
$f_\pi F_{eK}^P$	-1.832×10^{-3}
M_{eK}^T	$-1.432 \times 10^{-2} - i 3.226 \times 10^{-3}$
M_{eK}^P	$-8.466 \times 10^{-5} - i 1.894 \times 10^{-5}$

TABLE II: Enhancement effects in the $B^\pm \rightarrow K^{*0}\pi^\pm$ decay amplitudes

Scales	$\mu = t$ (~ 1.5 GeV)		$\mu = m_b/2$	
	Re (10^{-4} GeV)	Im (10^{-4} GeV)	Re (10^{-4} GeV)	Im (10^{-4} GeV)
$f_{K^*} F_e^T$	-1202.0	—	-1163.0	—
$f_{K^*} F_e^P$	45.9	—	35.6	—
$f_B F_a^T$	-350.1	44.2	-340.7	42.8
$f_B F_a^P$	20.0	-20.7	15.5	-14.8
M_e^T	-43.7	53.2	-33.8	41.1
M_e^P	3.1	-4.3	2.4	-3.3
M_a^T	-4.4	-13.0	-3.4	10.2
M_a^P	-0.3	0.0	-0.3	0.0
Br. with ann.	10.0×10^{-6}		6.0×10^{-6}	
Br. without ann.	4.6×10^{-6}		2.8×10^{-6}	

TABLE III: PQCD predictions and experimental data for the $B \rightarrow K^*\pi$ branching Ratios in unit of 10^{-6} .

Modes	CELO	Belle	BaBar	PQCD
$K^{*\pm}\pi^\mp$	$16^{+6.3}_{-5.4}$	26.0 ± 9.0	—	$9.1^{+4.9+0.3}_{-3.9-0.2}$
$K^{*0}\pi^\pm$	< 16	$16.2^{+4.8}_{-4.5}$	15.5 ± 3.8	$10.0^{+5.3}_{-3.5} \pm 0.0$
$K^{*\pm}\pi^0$	—	—	—	$3.2^{+1.9+0.6}_{-1.2-0.2}$
$K^{*0}\pi^0$	—	—	—	$2.8^{+1.6}_{-1.0} \pm 0.0$

\bar{B}_d^0 (B^-) meson lifetime $\tau_{B^0} = 1.55$ ps ($\tau_{B^-} = 1.65$ ps) [18]. The angle $\phi_3 = 80^\circ$ was extracted from the data of the $B \rightarrow K\pi$ and $\pi\pi$ decays [2, 8]. With all the meson wave functions given in our previous works, we calculate the contributions from all the topologies as shown in Figs. 2 and 3 in $B \rightarrow K\pi$ paper[2]. The allowed range of B-meson shape parameter, 0.36 GeV $< \omega_B < 0.44$ GeV, and chiral factor for pion, 1.2 GeV $< m_0^\pi < 1.6$ GeV is determined from the reasonable $B \rightarrow \pi$ and $B \rightarrow K$ transition form factors. For example, all amplitudes for the $B^+ \rightarrow K^{*+}\pi^0$ modes are listed in Table I, whose values are mostly the same magnitude for other decay channels, because the difference comes only from electroweak penguin contributions. We show in Table II the enhancing effect by comparing the decay amplitudes evaluated at the characteristic hard scales t in PQCD and $m_b/2$ in QCDF. It is also found that the annihilation contributions are sizable in two-body charmless B meson decays for the heavy-meson mass around 5 GeV [2] and in fact contributed about 60% fraction of the branching ratios, since factorized annihilation penguin contribution has large imaginary part and also the same order of magnitudes in real part as one of the factorized penguin contribution. As expected, the dominant factorizable penguin amplitudes are enhanced by about 30% due to the Wilson evolution, more than the factorizable tree amplitudes are. The PQCD predictions for the $B \rightarrow K^*\pi$ branching ratios, presented in Table III, are consistent with present experimental data. Here the first uncertainty comes from the allowed ranges of both ω_B and m_0^π , and the second one comes from the uncertainty of

$$R_b = |V_{ub}/V_{cb}|/\lambda.$$

Our predictions for the CP asymmetries in $B \rightarrow K^*\pi$ decays are given in Table IV, which have the same sign as of those in $B \rightarrow K\pi$ decays. For $\phi_3 = 80^\circ$, CP asymmetries of $B^0 \rightarrow K^{*0}\pi^\mp$ and $B^\pm \rightarrow K^{*0}\pi^\pm$ become large due to the important imaginary penguin annihilation amplitudes.

At last, the dependence of the branching ratios of $B^0 \rightarrow K^{*\pm}\pi^\mp$ and $B^\pm \rightarrow K^{*0}\pi^\pm$ on the angle ϕ_3 is shown in Fig.1 and large direct CP asymmetries of the

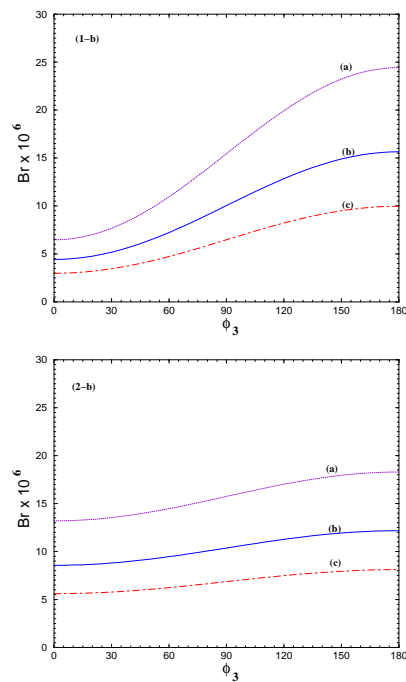


FIG. 1: Branching ratios of $B^0 \rightarrow K^{*\pm}\pi^\mp$ (1-b) and $B^0 \rightarrow K^{*0}\pi^\pm$ (2-b) versus ϕ_3 angle. The dot-, solid- and dashed-dot line stands for the averaged branching ratio with (a) $\omega_B = 0.36$ GeV and $m_0^\pi = 0.16$ GeV, (b) $\omega_B = 0.40$ GeV and $m_0^\pi = 0.14$ GeV, and (c) $\omega_B = 0.44$ GeV and $m_0^\pi = 0.12$ GeV, respectively.

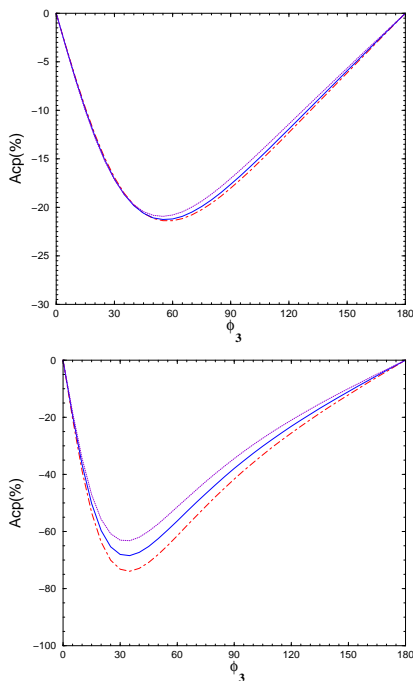


FIG. 2: Direct CP asymmetry in $B^0 \rightarrow K^{*\pm}\pi^\mp$ (upper) and $B^\pm \rightarrow K^{*\pm}\pi^0$ (lower).

$B^0 \rightarrow K^{*\pm}\pi^\mp$ and $B^\pm \rightarrow K^{*\pm}\pi^0$ on the angle ϕ_3 is exhibited in Fig.2. The branching ratios of $K^{*\pm}\pi^\mp$ and $K^{*\pm}\pi^0$ increase with ϕ_3 rapidly, while the $K^{*0}\pi^\pm$ and $K^{*0}\pi^0$ modes are insensitive to the variation of ϕ_3 . The increase with ϕ_3 is mainly a consequence of the interference between the penguin contribution F_e^P and the tree contribution F_e^T . The dependence on both the shape parameter w_B for the B meson wave function and the chiral factor m_0^π is also shown, which is strong in the $K^{*\mp}\pi^\pm$

and $K^{*\mp}\pi^0$ modes, and weak in the other two. The sensitivity is attributed to the fact that the former contain both F_e^P and F_e^T , which involve the B meson wave function, while the latter contain only F_e^P .

TABLE IV: Direct CP Asymmetry of the $B \rightarrow K^*\pi$ decays. Case A corresponds to $\omega_B = 0.44$ GeV, $m_0^\pi = 1.2$ GeV, Case B is to $\omega_B = 0.40$ GeV, $m_0^\pi = 1.4$ GeV, and Case C is to $\omega_B = 0.36$ GeV, $m_0^\pi = 1.6$ GeV.

Modes	case A	case B	case C	pQCD
$K^{*\pm}\pi^\mp$	-19.6 %	-19.2 %	-18.7 %	$-19.2^{+0.5}_{-1.7}$ %
$K^{*0}\pi^\pm$	-4.4 %	-3.6 %	-2.7 %	$-3.6^{+0.9}_{-0.8}$ %
$K^{*\pm}\pi^0$	-47.9 %	-43.7 %	-39.7 %	$-43.7^{+4.0}_{-4.2}$ %
$K^{*0}\pi^0$	-10.7 %	-9.6 %	-8.8 %	$-9.6^{+0.8}_{-1.1}$ %

In this letter in order to explain one of the hardly understandable processes in charmless B-decays, we have investigated the dynamical enhancement effect in the $B \rightarrow K^*\pi$ decays within pQCD method. Owing to the dynamical enhancement of penguin contributions at $t \sim 1.5$ GeV, pQCD predictions for all the $B \rightarrow K^*\pi$ modes are consistent with the present experimental data, which is a crucial decay process to distinguish pQCD from other approaches. We also predicted large direct CP asymmetry for $B^0 \rightarrow K^{*\pm}\pi^\mp$ about -20% and for $B^\pm \rightarrow K^{*0}\pi^\pm$ about -40%, which can be tested in near future measurements. More detail works will appear elsewhere[19].

We wish to thank S.J. Brodsky, H.Y. Cheng, H.-n. Li, A.I. Sanda and G. Zhu for helpful discussions. This work was supported by Grant-in-Aid for Scientific Research from Ministry of Education, Science and Culture of Japan.

-
- [1] H.-n. Li and H.L. Yu, Phys. Lett. B **353**, 301 (1995).
[2] Y.Y. Keum, H.-n. Li, and A.I. Sanda, Phys. Lett. B **504**, 6 (2001); Phys. Rev. D **63**, 054008 (2001); Y.Y. Keum and H.-n. Li, Phys. Rev. **D63**, 074006 (2001).
[3] C. D. Lü, K. Ukai, and M. Z. Yang, Phys. Rev. D **63**, 074009 (2001).
[4] C.-D. Lu and M.-Z. Yang, Eur. Phys. J. C **23**, 275 (2002)
[5] C.-H. Chen, Y.-Y. Keum and H.-N. Li, Phys. Rev. D **64**, 112002 (2001); S. Mishima, Phys. Lett. B **521**, 252 (2001);
[6] C.-H. Chen, Y.-Y. Keum and H.-N. Li, Phys. Rev. D **66**, 054013 (2002).
[7] C.H. Chen and H.-n. Li, Phys. Rev. D **63**, 014003 (2001).
[8] Y.Y. Keum, H.-n. Li, and A.I. Sanda, hep-ph/0201103; Y.Y. Keum and A.I. Sanda, hep-ph/0209014; Y.-Y. Keum, hep-ph/0209002; hep-ph/0209208 (Accepted in Phys. Rev. Lett.).
[9] J. Botts and G. Sterman, Nucl. Phys. B **225**, 62 (1989); H.-n. Li and G. Sterman, Nucl. Phys. B **381**, 129 (1992).
[10] G.P. Lepage and S.J. Brodsky, Phys. Lett. B **87**, 359 (1979); Phys. Rev. D **22**, 2157 (1980).
[11] M. Beneke, G. Buchalla, M. Neubert, and C.T. Sachrajda, Phys. Rev. Lett. **83**, 1914 (1999); Nucl. Phys. B **591**, 313 (2000).
[12] M. Beneke, hep-ph/0207228
[13] H.Y. Cheng and K.C. Yang, Phys. Rev. D **64**, 074004 (2001).
[14] H.Y. Cheng, Y.-Y. Keum and K.C. Yang, Phys. Rev. D **65**, 094023 (2002).
[15] M. Bauer, B. Stech, M. Wirbel, Z. Phys. C **29**, 637 (1985); Z. Phys. C **34**, 103 (1987).
[16] D. Du, J. Sun, D. Yang, and G. Zhu, Phys. Rev. D **65**, 074001 (2002); Phys. Rev. D **65**, 094025 (2002); hep-ph/0209233.
[17] N.G. Deshpande, X.G. He, W.S. Hou and, S. Pakvasa, Phys. Rev. Lett. **82**, 2240 (1999); W.S. Hou, J.G. Smith, and F. Würthwein, hep-ex/9910014.
[18] Review of Particle Physics, Eur. Phys. J. C **3**, 1 (1998).
[19] Y.-Y. Keum, in preparation.